EXPERIMENTAL AND NUMERICAL STUDY OF CONSTANT AREA MIXING

Václav Dvořák*, Tomáš Vít *
***Technical University in Liberec, Faculty of Mechanical Engineering,**
Department of Power Engineering Equipment
vaclav.dvorak@vslib.cz, tel: 485353479, fax: 485353644

Keywords: *ejector, constant area mixing, CTA, Fluent*

Abstract

The article deals with experimental and numerical study of constant area mixing in the cylindrical mixing chamber. We used Hot Wire Anemometry for experimental investigation and Fluent for numerical computations. We obtained curves of ejector performance and of ejector efficiency, profiles of velocity and of turbulence intensity in the mixing chamber and static pressure distribution on the wall of the mixing chamber. The results of experiments are compared with numerical data. We discussed accuracy and suitability of used turbulence models to calculate this particular phenomenon. The most suitable turbulence model seems to be realizable k-epsilon.

1 Introduction

Static pressure rises during constant area mixing. The optimal length of the cylindrical mixing chamber and the place where the mixing processes are finished as well is considered to be in the position of the maximum static pressure. The optimal length of the mixing chamber is sometimes taken as certain multiple of the chamber diameter [1]. It is evident that the mixing process strongly depends on the velocity ratio of both flows as we can see from equation (1) for the jet thickness $\bar{b}$ [2].

$$\bar{b} = \frac{b}{x} = C\frac{1+\bar{\rho}}{2}\frac{1-\omega}{1+\bar{\rho}\omega}. \qquad (1)$$

This work describes experimental and numerical investigation of constant area mixing in the cylindrical mixing chamber. The aim of this contribution is to find a suitable turbulence model that will support next research of mixing processes and subsequent analyses of parameters determining the finishing of mixing processes and optimal mixing chamber length for different ejector configurations and regimes.

2 Methods

The experimental object was an ejector with cylindrical mixing chamber of diameter $D = 40\ mm$ and length $L = 360\ mm$. The inlet area ratio was chosen $A_1 / A_2 = 0.3$, that is an optimum value according 1D theory [3]. Experimental ejector configuration, notation and system of coordinates are in Fig. 1.

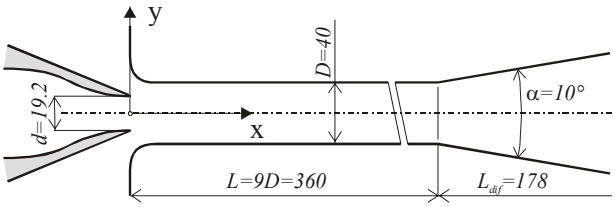

Fig. 1: Ejector configuration.

2.1 Experimental setup

Experimental setup is evident from Fig. 2. The high pressure primary air from a compressor was led through control valves to the primary stream nozzle; secondary steam was sucked from laboratory air. There was a diffuser behind the mixing chamber. The mass flow rate of primary stream was measured by rotameter and total mass flow rate through the ejector was measured by an orifice.

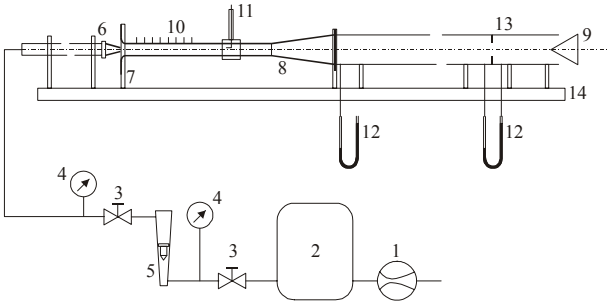

Fig. 2: Experimental setup: 1 - compressor, 2 - pressure tank, 3 - control valve, 4 - manometer, 5 - rota meter, 6 - primary nozzle, 7 - secondary nozzle, 8 - diffuser, 9 - choking, 10 - static pressure taps in the mixing chamber, 11- CTA probe holder, 12 - U-manometer, 13 - orifice, 14 - bed.

2.2 CTA measuring

Both single-sensor miniature wire probes DANTEC 55P11 (straight) and DANTEC 55P14 (right angle, perpendicular) connected with CA-1000 Connector Accessory Enclosure and with DANTEC 56C17 CTA anemometer bridge were used for velocity measurements. We used software DANTEC Streamline to evaluate the results. DANTEC 90H02 Flow unit was used for velocity calibration.
Owing to the used attachment of the probe and to the condition that the magnitude of radial component of velocity $U_y \to 0$, component of velocity vector measured by us will be interpreted as axial component of velocity U_x. Standard deviation from recorded velocity

$$\sigma_u^2 = \frac{\sum (U_i - \overline{U})^2}{n-1} \qquad (2)$$

is interpreted as the magnitude of the mean square of fluctuation part of velocity u'. In our case the probe is affected both by axial u'_x fluctuations and by radial component of fluctuation u'_y. Intensity of fluctuation can be than defined as

$$I_T = \frac{\sqrt{(u'^2)}}{\overline{U}_x} \; . \qquad (3)$$

Special traverse mechanism was constructed to reach high quality results. This traverse mechanism was fixed into the wall of the mixing chamber. The micrometer screw was used to adjust distance of the probe from the wall. The position of the probe was set with accuracy of 0.05 mm.

2.3 Numerical investigation

We used Fluent 6.1 and coupled solver to calculate compressible flow of ideal air in 2D axi-symmetric model of investigated ejector. Partially structured mesh of quadratic elements had about 80.000 cells. We tested five turbulence models: Spalart-Allmaras (*SA*), standard k-omega (*sko*), k-epsilon RNG (*keRNG*), realizable k-epsilon (*rke*) and Reynolds stress model (*RSM*).

3 Results

The ejector was investigated for gauge stagnation pressure of primary stream $p_{01} - p_{02} = 1 kPa$, while the absolute pressure was $p_{02} = p_{atm} \cong 98 kPa$. We measured mass flow rates for all achievable back pressures to obtain performance and efficiency curves of the ejector. We measured velocity and turbulence intensity profiles for regime of relative back pressure $\Pi = 0.17$.

3 Ejector performance and efficiency

There are curves of ejector performance in Fig. 3, where Π is relative back pressure

$$\Pi = \frac{p_b - p_{02}}{p_{01} - p_{02}} \; , \qquad (4)$$

where p_b is back pressure, p_{01} and p_{02} are stagnation pressures of primary stream and secondary stream, and

$$\Gamma = \frac{\dot{m}_2}{\dot{m}_1} \qquad (5)$$

is ejection ratio. The maximum value is $\Pi = 0.34$ for $\Gamma = 0$.

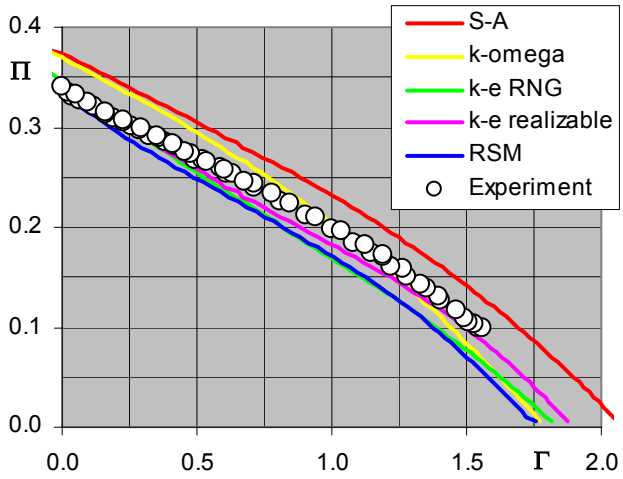

Fig. 3: Ejector performance.

Turbulence models *SA* and *sko* predict this value higher $\Pi = 0.37$, while other models are correct. For higher values of ejection ratio all models except for *SA* predict too low relative back pressure. These data are compiled into efficiency curves in Fig. 4. The ejector efficiency is defined as

$$\eta = \frac{\dot{m}_2}{\dot{m}_1} \frac{1-\left(p_{02}/p_b\right)^{\frac{\kappa-1}{\kappa}}}{\left(p_{01}/p_b\right)^{\frac{\kappa-1}{\kappa}}-1}. \qquad (6)$$

The highest measured value of ejector efficiency is 25% and prediction of *sko* corresponds to it. Model *SA* predicts higher efficiency 31%, while *keRNG* and *RSM* lower 21% and *rke* 22.5%. Only prediction of model *sko* corresponds to measured value, but the position of the top of the curve does not.

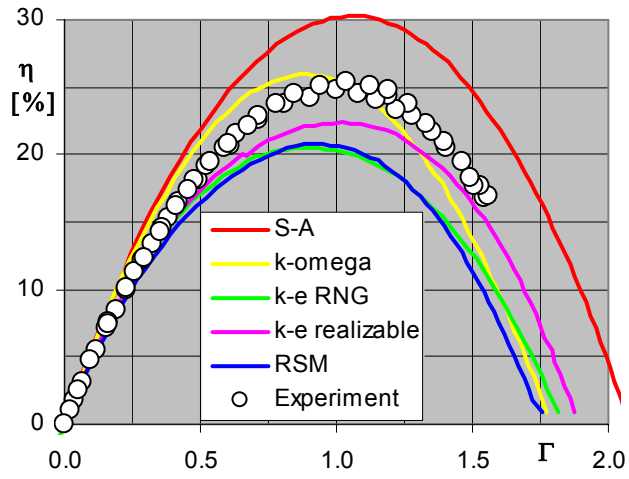

Fig. 4: Ejector efficiency.

3.2 Velocity and turbulence intensity profiles

Velocity profiles in the mixing chamber for two distances $x = 90\ mm$ and $x = 230\ mm$ behind the trailing edge of the primary stream nozzle are in Fig. 5 and Fig. 6. For the former distance all velocity profiles are similar except for these of model *SA* which predict higher velocity in the secondary flows. For the later distance, which corresponds to the position of the maximal turbulent kinetic energy, the variations of velocity profiles are more significant.

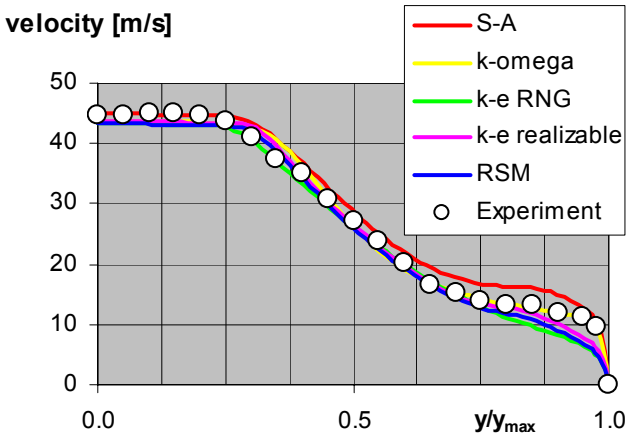

Fig. 5: Velocity profiles for $x = 90\,mm$.

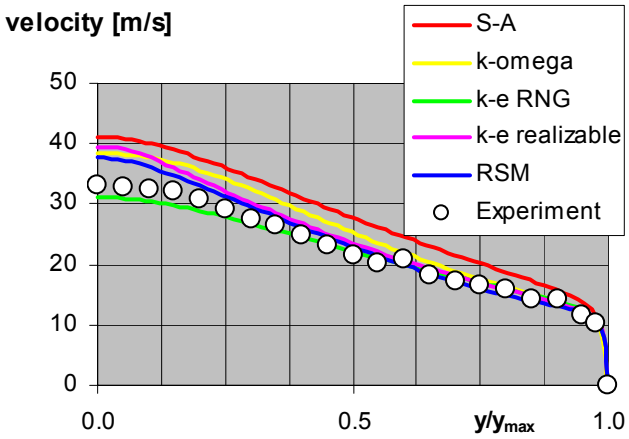

Fig. 6: Velocity profiles for $x = 230\ mm$.

Turbulence intensity profiles for two distances are in Fig. 7 and Fig. 8. Most of turbulence models predict turbulent kinetic energy k, while model *SA* predicts turbulent viscosity ν_T.

We used relation

$$I_T = \sqrt{\frac{2}{3}k}\,\frac{1}{U} \qquad (7)$$

to compute turbulence intensity from k and relation

$$I_T = \frac{\sqrt{\nu_T \dfrac{\partial U}{\partial y}}}{U}, \qquad (8)$$

to compute turbulence intensity from ν_T.

Turbulence model *SA* predicts significantly low turbulence intensity, while model *sko* gives unreal curve near the wall and in the primary stream. Experimental data lie between curves given by model *keRNG* and models *RSM* and *rke*.

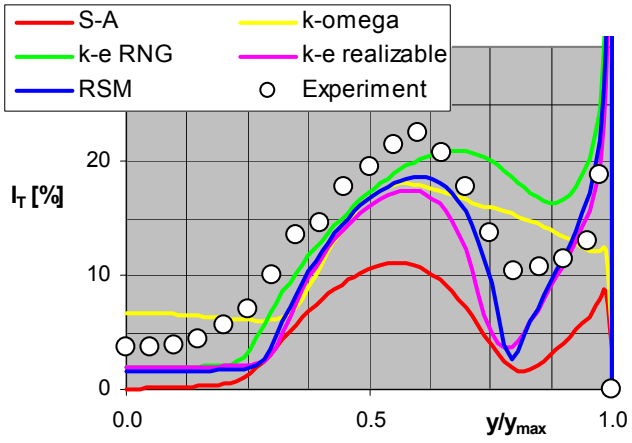

Fig. 7: Turbulence intensity for $x = 90\,mm$.

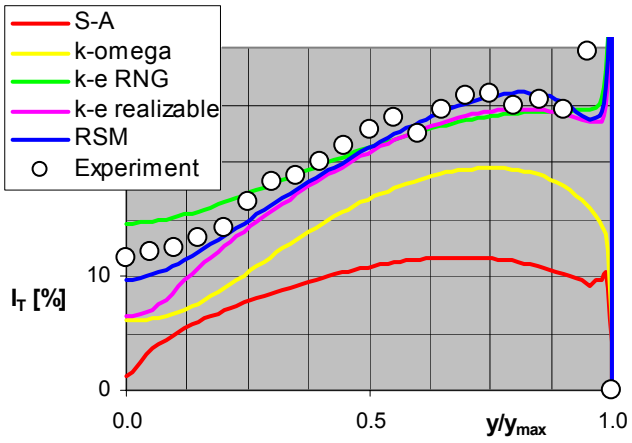

Fig. 8: Turbulence intensity for $x = 230\,mm$.

Other profiles of velocity and turbulence intensity in the mixing chamber obtained by experiments and compared with numerical computation using turbulence model realizable k-epsilon are in Fig. 10 and Fig. 11. We can see the growth of the mixing shear layer and transformation of velocity profile.

An example of results of numerical calculations obtained by using realizable k-epsilon model is in Fig. 12. We can see contours of velocity and of turbulence intensity in the mixing chamber. It is obvious how the region of the primary stream disappears and the mixing shear layer spreads behind the trailing edge of the primary nozzle.

3.3 Static pressure distribution

We can see how the static pressure rises during mixing. The distribution of static pressure on the wall of the cylindrical mixing chamber is in Fig. 9. Curves of two models - *rke* and *RSM* - are close to experiments, while curves of *SA* and *sko* are below and curve of *keRNG* is above experimental curve.

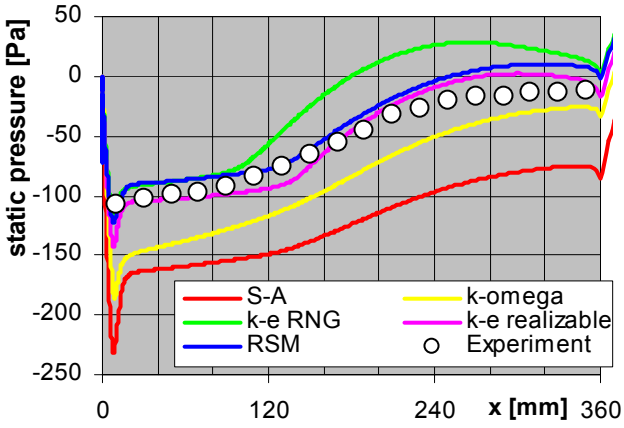

Fig. 9: Static pressure distribution on the wall of the mixing chamber for $\Pi = 0.17$.

4 Discussions

Suitability of used turbulence models to model mixing processes in investigated ejector follows from mentioned results. Turbulence model Spalart-Allmaras significantly overestimates the amount of sucked air of the

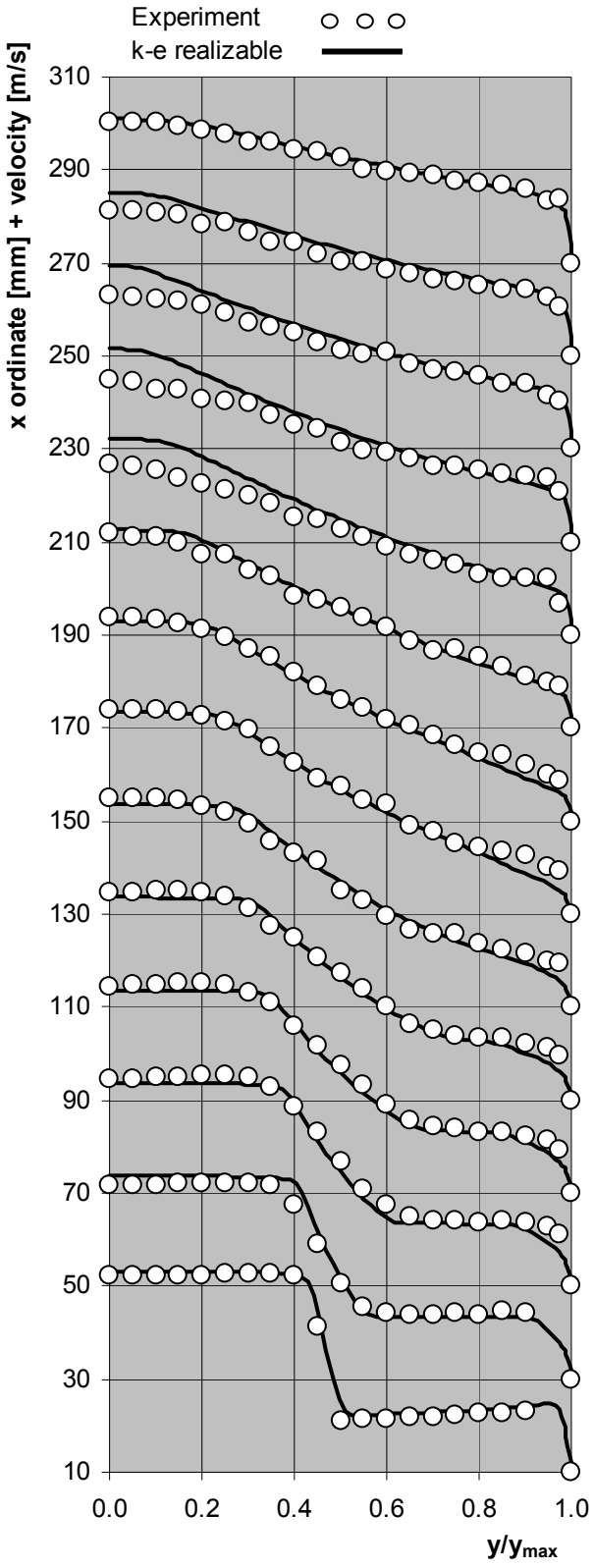

Fig. 10: Velocity profiles in the mixing chamber.

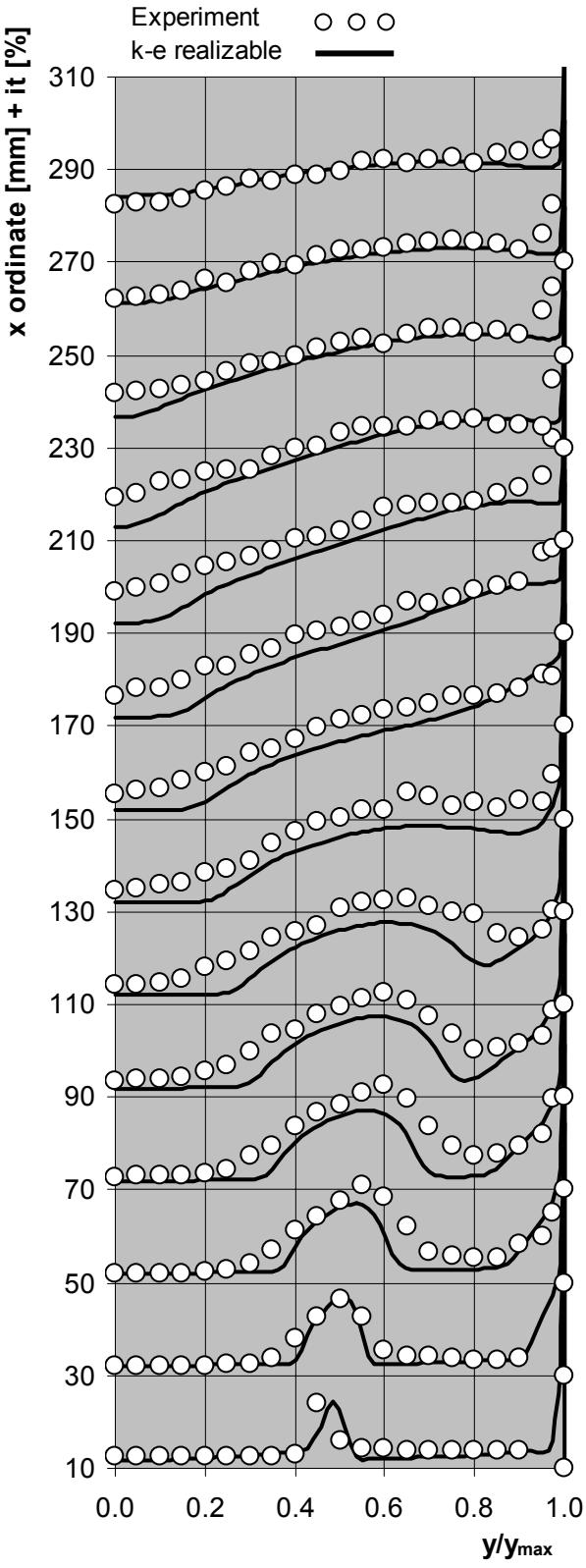

Fig. 11: Turbulence intensity profiles in the mixing chamber.

secondary stream and this feature yields higher velocity ratio ω and slowers mixing processes. It causes higher efficiency, deformed velocity profiles with faster secondary stream, lower turbulence intensity and lower static pressure in the mixing chamber.

Standard k-omega is only one turbulence model that predicts the value of the highest reached ejector efficiency, but both ejector curves - efficiency and performance are deformed. It seems, that model *sko* changes its accuracy by velocity ratio ω. Model *sko* gives unreal curve of turbulence intensity profile near the wall and in the primary stream. Static pressure in the mixing chamber is predicted lower than in reality.

Model k-epsilon RNG predict lower amount of air in the secondary stream for given relative back pressure and so lower efficiency. The velocity profiles correspond to measurements and also curves of turbulence intensity get near to reality. Static pressure is predicted correctly in the beginning of the mixing chamber, but rises too much then.

Reynolds stress model returns similar results as *keRNG* - curves of ejector efficiency and performance and velocity profiles, but also agrees better with experiments in turbulence intensity and in static pressure in the mixing chamber.

Turbulence model realizable k-epsilon predicts lower amount of sucked air of the secondary stream, but its curves of performance and efficiency agree best to the measurements. The other results, velocity, turbulence intensity and static pressures, are similar to results of *RSM*.

From this explanation we can say, that the worst turbulence model for modelling mixing processes in a cylindrical mixing chamber is Spalart-Allmaras. A little bit better is standard k-omega. There is k-epsilon RNG in the middle and RSM is quite good. Turbulence model realizable k-epsilon seems to be the best choice for this kind of problems.

5 Conclusions

The constant area mixing processes were studied with the support of the experimental and the numerical methods. We used Hot Wire Anemometry for experimental investigation and Fluent for numerical computations. We obtained curves of ejector performance and of ejector efficiency, profiles of velocity and of turbulence intensity in the mixing chamber and static pressure distribution on the wall of the mixing chamber. The results of experiments were compared with numerical data. We discussed accuracy and suitability of used turbulence models to calculate this particular phenomenon. The most suitable turbulence model seems to be realizable k-epsilon.

We would like to carry out several precise experiments using single inclined and X wire probes. Single inclined probe helps us to measure two components of the velocity vector. X wire probe will be used to obtain information about the distribution of shear stress and higher-order moments of turbulent flow. Realization of more accurate experiments near the wall and in the shear layer is also essential.

Results from these experiments should lead to the validation of the model as it is implemented into the software Fluent. We hope that our investigation brings new knowledge to the construction of ejectors and helps to design ejectors with better parameters.

Acknowledgments

This project was realized with financial support from the state resources by the Czech Science Foundation, grant no. 101/05/P298 "Optimization and control of mixing processes" and with financial support from MSM 4674788501. The authors wish to express their sincere gratitude for the professional help received from the research team of the Department of Power Engineering Equipment, TU in Liberec – Mr. J. Fridrich, Mr. J. Kneř and Mr. P. Jerje.

References

[1] Porter J L, Squyers R A. *A summary of ejector augmentor theory and performance.* ATC Report No. R-91100/9CR-47A, Vought Corpn Advanced Technology Cr, Dallas, Texas, 1981.

[2] Abramovich, G. N. *The theory of turbulent jets*. The Massachusetts Institute of Technology, USA, 1963.

[3] Dvořák V.: Parameters for Classification and Optimisation of Ejectors. In: Topical Problems of Fluid Mechanics 2005, IT ASCR, February 16 - 17, 2005, pp. 31 - 34, Praha, Czech Republic, 2005. ISBN 80-85918-92-7.

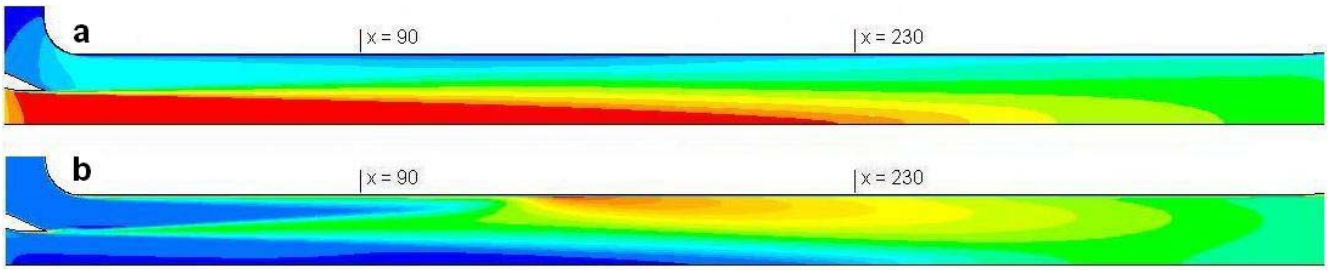

Fig. 12: Numerical calculation, k-ε realizable model, contours: a - velocity, b - turbulence intensity.